NJC

Accepted Manuscript

Volume 1 | Number 1 | Jan 2013 | Pages 1–100

NJC

New Journal of Chemistry

www.rsc.org/njc

A journal for new directions in chemistry

ROYAL SOCIETY OF CHEMISTRY

ROYAL SOCIETY OF CHEMISTRY

www.rsc.org/njc

New Journal of Chemistry

Cite this: DOI: 10.1039/c0xx00000x

www.rsc.org/xxxxxx

ARTICLE TYPE

Peroxo- and oxovanadium (IV) complexes with tridentate N-heterocycle ligands: synthesis, structure, and catalytic performance

Xi Tong Ma, Na Xing*, Zhi Dan Yan, Xiao Xi Zhang, Qiong Wu, Yong Heng Xing*

Received (in XXX, XXX) Xth XXXXXXXXX 20XX, Accepted Xth XXXXXXXXX 20XX

DOI: 10.1039/b000000x

Three peroxo- and oxovanadium (IV) complexes: $[VO(O_2)$ (bpz*eaT)$\cdot VO(C_4H_4O_6)]\cdot H_2O$ (**1**), $[VOSO_4$(bpz*eaT)$]\cdot C_6H_8O_7$ (**2**) (bpz*eaT= 2,4-bis(3,5-dimethyl-1*H*-pyrazol-1-yl)-6-diethylamino-1,3,5-triazine) and $[VO(C_{12}H_8N_2)(C_9H_7\ NO_3)]\cdot CH_3OH\cdot 0.5H_2O$ (**3**) were synthesized and characterized by elemental analysis, IR spectra, UV-Vis spectroscopy and single-crystal X-ray diffraction. In addition, the catalytic performances of complexes **1-3** and their starting materials (VO(acac)$_2$ and $VOSO_4$) were studied by the reaction of cyclohexane (Cy) oxidation. It is found that complex **1** exhibited the highest catalytic activity ($TON_{(cyclohexanol)}$=220, $TON_{(cyclohexanone)}$= 346, Conv.= 97.9%) with H_2O_2 as oxidant and HNO_3 as additive at 24 h, 40 ^oC, indicating that the complexes possess potential candidate catalysts to oxidize the Cy to cyclohexanol (CyOH) and cyclohexanone (CyO) in mild conditions.

Introduction

Cyclohexane (Cy) oxidation is one of the basic processes for producing cyclohexanol (CyOH) and cyclohexanone (CyO)[1] – these compounds are widely used in synthetic caprolactam, rubber, paints and organic solvents.[2,3] Conventionally, the oxidation process is carried out in homogeneous medium at elevated temperature (423-433K) and high pressure (1-2 MPa) using cobalt or metal-boric acid catalysts.[4] But this process suffers from the disadvantages like strict conditions, low conversion and environmental hazards.[5] Therefore, many attentions have been focused on the development of new catalysts under milder reaction conditions.

In recent years, vanadium complexes have been widely used in alkane oxidation owing to their high activities.[6-12] VOL_2 (L= 2-{(E)-[2-chloroethyl)imino] methyl}-6-methoxy phenol) exhibited high catalytic activity in the epoxidation of cyclooctene with TBHP as oxidant, which conversion was obtained 86%.[6] $[VOCl_2\{HOCH_2C(pz)_3\}]$ showed good catalytic activity (TON=405) in the Cy oxidation with H_2O_2 as oxidant.[7] High conversion (99.2%) was achieved promoted by vanadium complex, μ-Oxido-bis({R(−)-2-[(2-oxidopropyl) iminomethyl]-4-nitrophenolato-κ^3 N,O,O'}oxidovanadium(V)) with TBHP as oxidant in the oxidation of styene.[8] In general, those oxidovanadium complexes composed by V=O moiety and O, N donor ligands always show high catalytic activities in oxidation processes.[13-15]

Heterocycles containing nitrogen, such as pyrazole ring, 1,3,5-triazine ring or Schiff-base ligands has been paid considerable attention for their important roles in agrochemistry, drugs and polymers.[16-18] Among them, the 1,3,5-triazine derivatives and amino-Schiff-base ligands are frequently used in complex synthesis due to their abundant coordinated sites and easily preparation. The 1,3,5-triazine derivatives are particular aromatic moiety with a very strong electron-deficient character that allows the formation of π-π stacking and anion-π interactions. Amino-Schiff-base ligands may tune sterically and electronically by the variation of corresponding amino-acid aldehyde ligand precursors. X. Wang *et al.* synthesized five novel d^7-d^{10} complexes Cu, Co, Ni with 1,3,5-triazine-pyrazolyl as ligand and studied their surface photovoltage properties.[19] C. Chen *et al.* explored the catalytic bromination activities of vanadium (III, IV and V) complexes with pincer N-heterocycle ligands.[20] However, few results have been reported about the synthesis of peroxo- and oxovanadium(IV) complexes with 1,3,5-triazine-pyrazolyl and polycarboxylate as ligands together, especially their activities in Cy oxidation.

In this paper, we successfully synthesized three vanadium (IV) complexes, $[VO(O_2)$(bpz*eaT)$\cdot$ $VO(C_4H_4O_6)]\cdot H_2O$ (**1**), $[VOSO_4$ (bpz*eaT)$]$ $\cdot C_6H_8O_7$ (**2**) and $[VO(C_{12}H_8N_2)(C_9H_7 NO_3)]\cdot CH_3OH\cdot 0.5H_2O$ (**3**) with tridentate N-heterocyclic ligands (namely, 2,4-bis(3,5-dimethyl-1*H*-pyrazol-1-yl)-6-diethyl amino-1,3,5-triazine (bpz*eaT) shown in **scheme 1**) for the first time and defined their structures by the X-ray crystallography method. In particular, the three complexes were applied in the catalytic oxidation of Cy.

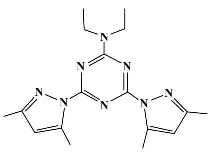

Scheme 1 bpz*eaT

Experimental

Materials and methods

All the chemicals used were of analytical grade and without further purification. Bpz*eaT[21,22] and KHL[23] were synthesized according to the modified literature method. Elemental analyses for C, H and N were carried out on a Perkin Elmer 240C automatic analyzer. Infrared spectra were recorded on a JASCO FT/IR-480 spectrometer with pressed KBr pellets in the range of 200-4000 cm^{-1}. UV-vis spectra were determined by a JASCO V-570 UV-Vis spectrometer (200–1500 nm, as solids). 30% aqueous solution of H_2O_2 was used as primary oxidant in the oxidation reactions. The products of Cy oxidation were analyzed by a GC-9790 series gas chromatograph equipped with a flame ionization detector (FID) and a capillary column (PG2000, column length: 30 m; internal diameter: 0.25 mm).

Synthesis of $[VO(O)_2(bpz*eaT)\cdot VO(C_4H_4O_6)]\cdot H_2O$ (1) $VO(acac)_2$ (0.25 mmol, 0.066 g), bpz*eaT (0.25 mmol, 0.085 g) and $C_4H_6O_6$ (0.5 mmol, 0.075 g) were dissolved in a solution of EtOH (12 mL), H_2O (1 mL) and one drop of H_2O_2, instantaneously giving a brown-yellow solution. After stirring for 4 h, the solution was left at room temperature for two days and turned to a red solution. Continued to be placed for several days, red crystals were obtained in *ca.* 64.28% yield based on V(IV). Anal. calc. for $C_{21}H_{32}N_8O_{11}V_2$: C, 37.38; H, 4.71; N, 16.64. Found: C, 37.36; H, 4.74; N, 16.61%. IR (KBr, cm^{-1}): 3439, 3117, 2970, 2930, 2872, 1659, 1610, 1493, 1454, 984, 1141, 1053, 559, 488.

Synthesis of $[VOSO_4(bpz*eaT)]\ \cdot C_6H_8O_7$ (2) $VOSO_4$ (0.25 mmol, 0.041 g), bpz*eaT (0.25 mmol, 0.085 g) and $C_6H_8O_7$ (0.5 mmol, 0.105 g) were mixed and kept stirring for 4 h in 12 mL of CH_3CN to get a blue solution. Then, the mixture was sealed into a glass vial and heated at 80°C for 1 day. After cooled to room temperature, blue crystals of **2** were obtained in *ca.* 70.22% yield based on V(IV). Anal. calc. for $C_{23}H_{32}N_8O_{12}SV$: C, 39.67; H, 4.62; N, 16.13. Found: C, 39.68; H, 4.60; N, 16.10 %. IR (KBr, cm^{-1}): 3511, 3120, 2977, 1761,1724, 1663, 1614, 1479, 1455, 1218, 1121, 1048, 988.

Synthesis of $[VO(C_{12}H_8N_2)(C_9H_7NO_3)]\cdot CH_3OH\cdot 0.5H_2O$ (3) $VOSO_4$ (0.25 mmol, 0.041 g), KHL (0.25 mmol, 0.055 g) and 1,10-phenanthroline ($C_{12}H_8N_2$) (0.25 mmol, 0.050 g) were dissolved in MeOH (12 mL). After stirring for 4 h, a deep orange solution was got. Then, 2 drops of water was added into it. After leaving at room temperature for a few days, deep orange-red crystals suitable for X-ray diffraction were obtained in *ca.* 67.52% yield based on V(IV). Anal. calc. for $C_{22}H_{18}N_3O_{5.5}V$: C, 56.95; H, 3.90; N, 9.08. Found: C, 56.98; H, 3.88; N, 9.06%. IR (KBr, cm^{-1}): 3441, 3056, 1631, 1627, 1432, 1148, 1070, 1021, 953.

X-ray Crystallographic Determination

Suitable single crystals of the complexes were mounted onto glass fibers for X-ray measurements. The reflection data were collected at room temperature on a Bruker AXS SMART APEX II CCD diffractometer with graphite monochromatized Mo-Kα radiation (λ = 0.71073 Å) and a ω scan mode. All the measured independent reflections ($I > 2\sigma(I)$) were used in the structural analyses and semi-empirical absorption corrections were applied using SADABS program.[24] The structures were solved by the direct method using SHELXL-97.[25] The crystallographic data and the structure refinements are given in **Table 1**.

Table 1 Crystallographic data for complexes **1, 2** and **3**.

Complex	**1**	**2**	**3**
Formula	$C_{21}H_{30}N_8O_{11}V_2$	$C_{23}H_{32}N_8O_{12}SV$	$C_{22}H_{18}N_3O_{5.5}V$
M(g mol^{-1})	672.41	695.57	463.34
Crystal system	Triclinic	Triclinic	Rhombohedral
Space group	*P-1*	*P-1*	*R-3*
a (Å)	9.616(6)	9.9813(13)	21.563(4)
b (Å)	12.119(7)	12.3482(15)	21.563(4)
c (Å)	12.594(7)	13.2980(17)	24.140(8)
α (°)	90.497(10)	103.220(2)	90
β (°)	98.270(10)	93.546(2)	90
γ (°)	113.050(9)	100.630(2)	120
V (Å^3)	1333.0(14)	1558.9(3)	9720(4)
Z	2	2	9
D_{calc}(g.m^{-3})	1.675	1.482	1.425
Crystal size (mm^3)	0.20 × 0.11 × 0.09	0.24 x 0.12 x 0.08	0.25 x 0.16 x 0.14
F(000)	692	722	4284
μ(Mo-Kα) (cm^{-1})	0.776	0.457	0.500
Reflections collected	6781	8039	19844
Independent reflections ($I > 2\sigma(I)$)	4665	5452	5389

Parameters	379	406	284
$\Delta(\rho)$ (e Å^{-3})	1.211 and -0.563	0.373 and -0.421	0.800 and -0.507
Goodness-of-fit	1.078	0.986	1.043
R_1[a]	0.0482 (0.0644)[b]	0.0443 (0.0740)[b]	0.0632 (0.0874)[b]
wR_2[a]	0.1295 (0.1367)[b]	0.0998 (0.1089)[b]	0.1720 (0.2031)[b]

[a] $R = \Sigma||Fo|-|Fc||/\Sigma|Fo|$, $wR_2 = [\Sigma(w(Fo^2-Fc^2)^2/\Sigma(w(Fo^2)^2]^{1/2}$; $[Fo > 4\sigma(Fo)]$.

[b] Based on all data.

Catalytic oxidation reaction

The catalytic experiment was carried out in a two-necked glass flask, placed in a water bath of 40 °C with magnetic stirring. In a typical experiment, a reaction solution mixed with 0.0004 g of the catalyst, the required amounts of Cy, H_2O_2, HNO_3 and 3 mL of acetonitrile was stirred under atmospheric pressure. 1.5 mL of diethyl ether was added to terminate the oxidation reaction. The extracted reaction mixture was analyzed by GC equipped detector by internal standard method with 0.03 g (3.26×10^{-4} mol) of methylbenzene as internal standard. The identification of the oxidation products was performed by comparing their retention times with that of the commercial CyOH and CyO.

Results and discussion

Synthesis

By analyzing the preparation process of the complexes **1, 2** and **3** (as shown in **Scheme 2**), it is found that the starting materials are different. $VO(acac)_2$ was used for **1**, while $VOSO_4$ was used for **2** and **3**. The complex **1** was synthesized in the mixed solution of ethanol-water-H_2O_2, while complex **2** was in the CH_3CN and complex **3** was in the methanol. Complexes **1** and **3** were synthesized at room temperature, while complex **2** was finished at 80°C. It was worth to mention that, we only obtained the powder of complexes **1** and **2** by changing the molar ratio of $VO(acac)_2$/bpz*eaT/tartaric acid or citric acid to 1: 1: 2 instead of 1: 1: 1 or 1: 1: 3. For complex **3**, the systematic experiments have been carried out by changing different starting materials e.g. $VO(acac)_2$, $VOSO_4$ and different molar ratio of $VOSO_4$/KHL (L: salicylideneglycinyl)/1,10-phenanthroline e.g. 2: 1: 1, 1: 1: 1 or 1: 1: 2 to find out their optimum reaction conditions. Through the results of these experiments, we found that not only is the temperature of the reaction a very sensitive reaction parameter, but also the molar ratio of starting materials seem to be important factor for preparation of the complexes. Detail IR and UV-Vis spectra data are provided in supplement material.

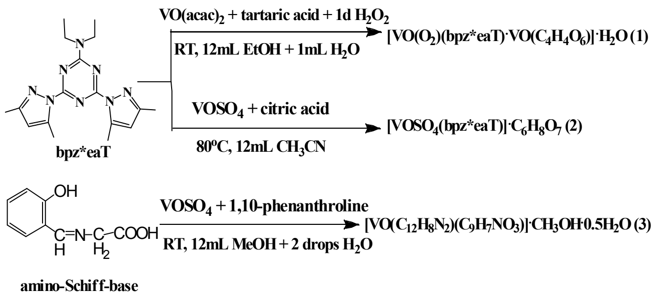

Scheme 2 The synthetic routes of complexes **1-3**.

Structural description of complexes 1-3

The molecular structures of complexes **1-3** are depicted in **Figs. 1-3**. Some selected bond distances, bond angles and hydrogen bonds are summarized in **Tables 2-3**.

X-ray single crystal analysis shows that the complex **1** (shown in **Fig. 1a**) is crystallized in the Triclinic system with *P-1* space group. The molecular structure contains two parts, and one lattice water molecule. One part is completed by one vanadium atom (V1), one terminal oxygen atom, one peroxo group and one bpz*eaT ligand. The other part contains two vanadium atoms (V2, V2#), two terminal oxygen atoms and two tartaric acid ligands. One vanadium atom (V1) is coordinated by one terminal oxygen atom (O1), three nitrogen atoms (N1, N6 and N8) from bpz*eaT ligand and two oxygen atoms (O3 and O4) from peroxo group. The other vanadium atom (V2) is coordinated by one terminal oxygen atom (O2) and four oxygen atoms (O5, O7, O8 and O10) from tartaric acid ligand. The bond lengths of V1-N are in the range of 2.065(3)-2.136(3) Å. The V1-O1 and V2-O2 bond lengths are 1.580(3) and 1.579(3) Å, respectively. The bond lengths of V1-O (3, 4) and V2-O (5, 7, 8 and 10) are in the range of 1.822(3)-1.822(3) and 1.790(3)-1.960(3) Å, respectively. The O-V-N, O-V-O and N-V-N angles are in the range of 83.72(14)-145.28(15), 43.48(15)-141.95(13) and 72.34(12)-144.80(11)°, respectively. In addition, there is an important C-H…O hydrogen bond (3.1917 Å) in complex **1**, as illustrated in **Fig. 1b**. The hydrogen bond comes from the methyl in pyrazolyl ring (C5) of the bpz*eaT ligand and the peroxo group ($O3^{\#1}$, #1: 1+x, y, z), which linked the independent molecules to form a 1D chain. There are also two intermolecular hydrogen bonds between the methyl in pyrazolyl rings (C1, C17) and the peroxo group (O4, O3).

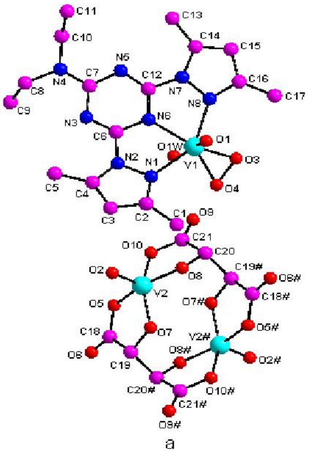

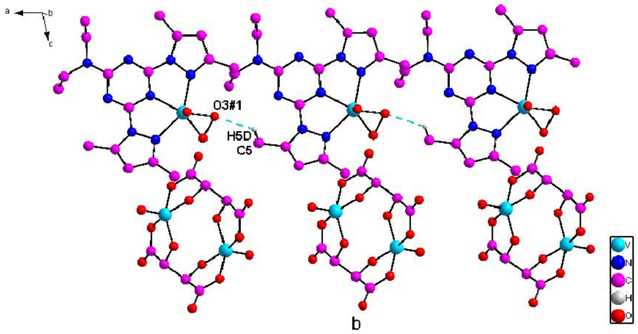

Fig. 1 (a) The molecular structure of complex **1** (All hydrogen atoms are omitted for clarity). (b) A view of one-dimensional hydrogen bonding network in complex **1** (All hydrogen atoms except for the hydrogen bonds are omitted for clarity).

Structural analysis indicates that the complex **2** (shown in **Fig. 2a**) is crystallized in the Triclinic system with *P-1* space group. The asymmetric unit of **2** is completed by one vanadium atom, one coordinated bpz*eaT ligand, one sulfate group and one lattice citric acid molecule. The coordination mode of the bpz*eaT ligand is similar to that of complex **1**, acting as a pincer tridentates ligand. The vanadium atom is coordinated by one terminal oxygen (O1), two oxygen atoms (O2, O3) from the sulfate group and three nitrogen atoms (N1, N6, N8) from the bpz*eaT ligand. The bond lengths of V-N are in the range of 2.012(2)-2.136(3) Å. The V-O1 bond length is 1.579(2) Å, while the distances of V-O2 and V-O3 are 2.0237(19) and 2.240(2) Å, which indicates that V-O1 is a double bond and V-O2 and V-O3 are single bonds. Furthermore, the distances of the coordinated S-O2 (1.507(2) Å) and S-O3 (1.5043 (19) Å) are slight longer than that of the uncoordinated S-O4 (1.448(2) Å) and S-O5 (1.432(2) Å). The O-V-N, O-V-O and N-V-N angles are in the range of 84.47(9)-150.98(9), 65.51(7)-163.39(10) and 74.20(9)-147.72(9)°, respectively. In addition, there are two kinds of hydrogen bonds, O-H…O (2.5970 Å, 2.6671 Å) and C-H…O (3.2644 Å, 3.3557 Å). Hereinto, the O-H…O comes from one lattice citric acid molecule and another lattice citric acid molecule: O10-H10D…$O11^{\#2}$ (2.6671 Å, #2: 1-x, 1-y, 1-z); the C-H…O is from the carbon atom of the bpz*eaT ligand, oxygen atom of the lattice citric acid molecule, carbon atom of the lattice citric acid molecule and oxygen atom of the uncoordinated sulfate group: C3-H3B…$O7^{\#3}$ (3.3557 Å, #3: 1-x, -y, -z) and C22-H22A…$O5^{\#4}$ (3.2644 Å, #4: 1-x, -y, 1-z). The molecule is linked through the O10-H10D…O11 and C3-H3B…O7 hydrogen bonds to generate a 1D chain structure, as illustrated in **Fig. 2b**, and then the adjacent chains are connected through C22-H22A…O5 hydrogen bond to form a 2D sheet structure, as showed in **Fig. 2c**. There is also a intermolecular hydrogen bond between the oxygen atom of the lattice citric acid molecule and oxygen atom of the coordinated sulfate group: O6-H6A…O3 (2.5970 Å).

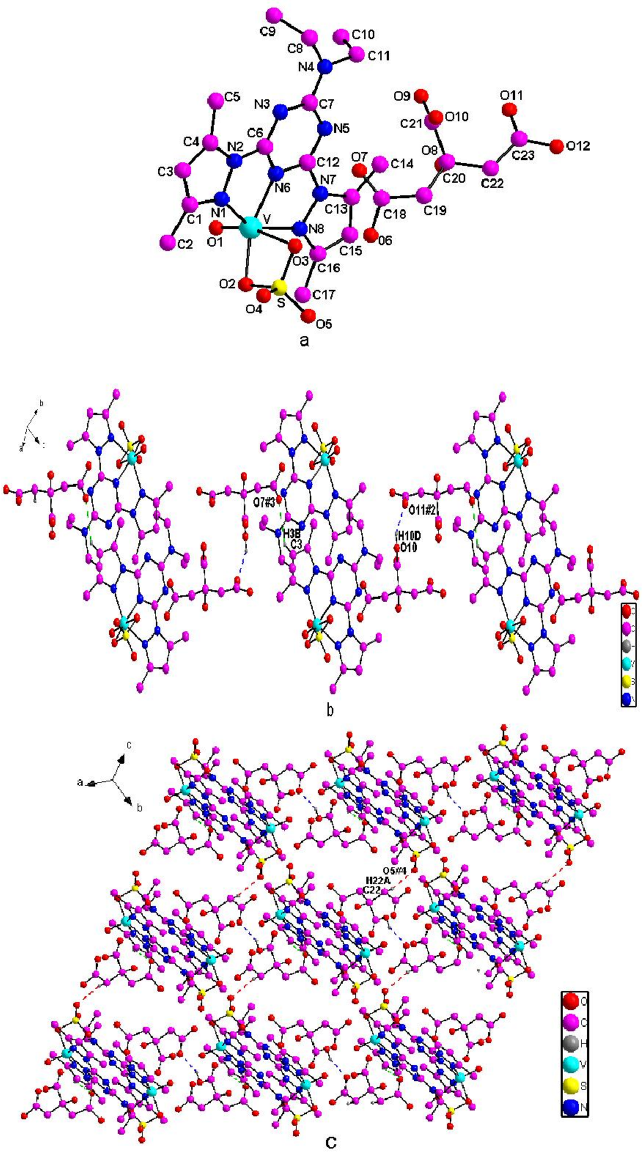

Fig. 2 (a) The molecular structure of complex **2** (All hydrogen atoms are omitted for clarity). (b) A view of one-dimensional hydrogen bonding network in complex **2** (All hydrogen atoms except for the hydrogen bonds are omitted for clarity). (c) A view of two-dimensional hydrogen bonding network in complex **2** (All hydrogen atoms except for the hydrogen bonds are omitted for clarity).

X-ray single crystal analysis indicates that the complex **3** is crystallized in the Rhombohedral system with *R-3* space group. The asymmetric unit of **3** is completed by one vanadium atom, one coordinated 1,10-phenanthroline, one tridentate Schiff-base ligand, one free methanol molecule and half of water molecule. As is shown in **Fig. 3a**, the central V atom is bonded with one terminal oxygen (O1), two nitrogen atoms (N1, N2) from 1,10-phenanthroline and two oxygen atoms, one nitrogen atom (O2, N4, O4) from the Schiff-base ligand. The bond lengths of V-N are in the range of 2.051(2)-2.376(2) Å. The V-O1 bond length is 1.594(2) Å. The bond lengths of V-O2 and V-O4 are 1.950(2) and 2.008(2) Å, respectively. The O-V-N, O-V-O and N-V-N angles are in the range of 79.22(9)-167.49(10), 98.88(11)-159.18(10) and 72.36(8)-159.05(10) Å. In addition, there is a C-H…O hydrogen bond (3.3484 Å) in complex **3**, as illustrated in **Fig. 3b**. The hydrogen bond comes from the carbon atom (C19) and oxygen atom (O4$^{\#5}$, #5: y, 1-x+y, 2-z) both from the Schiff-base ligand, which forms a 1D chain.

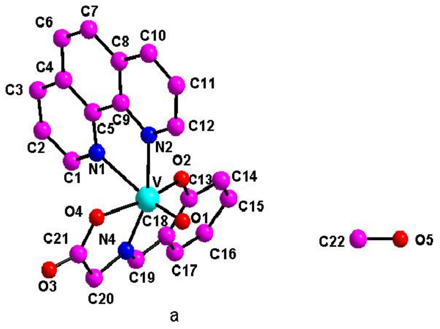

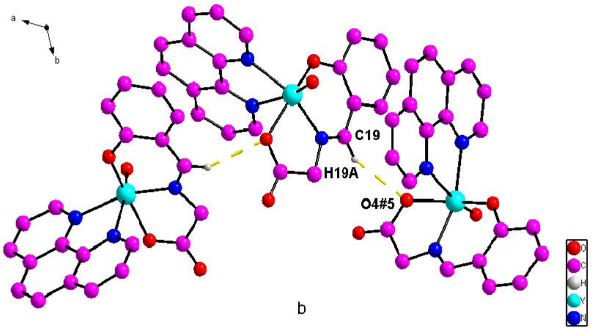

Fig. 3 (a) The molecular structure of complex 3 (All hydrogen atoms are omitted for clarity). (b) A view of one- dimensional hydrogen bonding network in complex 3 (All hydrogen atoms except for the hydrogen bonds are omitted for clarity).

Comparison of the structures By comparison, it is found that the bond lengths of V-N$_{pz}$ in complex **1** and **2** are slightly longer than V-N$_{triaz}$. The V-N$_{Schiff}$ and V-O$_{phenoxyl}$ bond distances are shorter than V-N$_{1,10\text{-}phen}$ and V-O$_{carboxyl}$, respectively, in complex **3**. The bond distances of V-O$_{sulfate}$ in complex **2** are 2.0237(19) and 2.240(2) Å, respectively. It is similar to those reported in the literature.[20]

Table 2 Selected bond distances and angles of complexes**1**, **2** and **3**.

Complex **1**					
V(1)-O(1)	1.580(3)	O(1)-V(1)-O(3)	103.15(19)	N(1)-V(1)-N(8)	144.80(11)
V(1)-O(4)	1.822(3)	O(4)-V(1)-O(3)	43.48(15)	O(2)-V(2)-O(8)	104.12(16)
V(1)-O(3)	1.836(4)	O(1)-V(1)-N(6)	104.69(16)	O(2)-V(2)-O(7)	107.00(15)
O(3)-O(4)	1.368(5)	O(4)-V(1)-N(6)	145.28(15)	O(8)-V(2)-O(7)	98.88(12)
V(1)-N(6)	2.065(3)	O(3)-V(1)-N(6)	144.16(15)	O(2)-V(2)-O(5)	101.52(16)
V(1)-N(1)	2.127(3)	O(1)-V(1)-N(1)	92.24(15)	O(8)-V(2)-O(5)	152.97(13)
V(1)-N(8)	2.136(3)	O(4)-V(1)-N(1)	85.21(15)	O(7)-V(2)-O(5)	81.49(12)
V(2)-O(2)	1.579(3)	O(3)-V(1)-N(1)	128.29(15)	O(2)-V(2)-O(10)	109.94(15)
V(2)-O(8)	1.790(3)	N(6)-V(1)-N(1)	72.58(13)	O(8)-V(2)-O(10)	80.81(12)
V(2)-O(7)	1.822(3)	O(1)-V(1)-N(8)	93.86(15)	O(7)-V(2)-O(10)	141.95(13)
V(2)-O(5)	1.939(3)	O(4)-V(1)-N(8)	126.85(16)	O(5)-V(2)-O(10)	82.59(12)
V(2)-O(10)	1.960(3)	O(3)-V(1)-N(8)	83.72(14)	O(4)-O(3)-V(1)	67.7(2)
O(1)-V(1)-O(4)	102.47(18)	N(6)-V(1)-N(8)	72.34(12)	O(3)-O(4)-V(1)	68.5(2)
Complex **2**					
V-O(1)	1.579(2)	O(1)-V-O(2)	97.93(10)	O(2)-V-N(8)	103.63(9)
V-N(6)	2.012(2)	N(6)-V-O(2)	150.98(9)	N(1)-V-N(8)	147.72(9)
V-O(2)	2.0237(19)	O(1)-V-N(1)	99.50(11)	O(1)-V-O(3)	163.39(10)
V-N(1)	2.103(2)	N(6)-V-N(1)	74.54(9)	N(6)-V-O(3)	85.55(8)
V-N(8)	2.118(2)	O(2)-V-N(1)	99.75(9)	O(2)-V-O(3)	65.51(7)
V-O(3)	2.240(2)	O(1)-V-N(8)	98.98(11)	N(1)-V-O(3)	85.31(9)
O(1)-V-N(6)	111.05(10)	N(6)-V-N(8)	74.20(9)	N(8)-V-O(3)	84.47(9)
Complex **3**					
V-O(1)	1.579(2)	O(1)-V-O(4)	98.88(11)	O(4)-V-N(2)	91.25(9)
V-N(6)	2.012(2)	O(2)-V-O(4)	159.18(10)	N(4)-V-N(2)	159.05(10)
V-O(2)	2.0237(19)	O(1)-V-N(4)	104.59(11)	O(1)-V-N(1)	167.49(10)

V-N(1)	2.103(2)	O(2)-V-N(4)	88.93(9)	O(2)-V-N(1)	82.31(9)
V-N(8)	2.118(2)	O(4)-V-N(4)	79.22(9)	O(4)-V-N(1)	80.17(9)
V-O(3)	2.240(2)	O(1)-V-N(2)	95.24(10)	N(4)-V-N(1)	87.55(9)
O(1)-V-N(6)	111.05(10)	O(2)-V-N(2)	94.07(8)	N(2)-V-N(1)	72.36(8)

Table 3 Hydrogen bonds (Å) of complexes **1**, **2** and **3**.

D–H···A	d(D–H)/ Å	d(H···A)/ Å	d(D···A)/ Å	∠D–H···A/ °
		Proposed hydrogen bonds for complex **1**		
C5-H5D···O3$^{\#1}$	0.9600	2.4695	3.1917	131.91
C1-H1A··· O4	0.9600	2.2629	3.0557	139.32
C17-H17A···O3	0.9600	2.2060	2.9860	137.60
		Proposed hydrogen bonds for complex **2**		
O10-H10D···O11$^{\#2}$	0.8500	1.8887	2.6671	151.56
C3-H3B···O7$^{\#3}$	0.9300	2.5728	3.3557	142.12
C22-H22A···O5$^{\#4}$	0.9700	2.4093	3.2644	146.80
O6-H6A···O3	0.8500	1.7696	2.5970	163.93
		Proposed hydrogen bonds for complex **3**		
C19-H19A···O4$^{\#5}$	0.9300	2.4972	3.3484	152.27

Symmetry transformation used to generate equivalent atoms: #1: 1+x, y, z; #2: 1-x, 1-y, 1-z; #3: 1-x, -y, -z; #4: 1-x, -y, 1-z, #5: y, 1-x+y, 2-z

Spectroscopic characterization

IR spectral studies The IR spectra of the complexes **1-3** are shown in **Figs. S1-S3** and the selected data are listed in **Table 4**. The broad absorption band appearing at around 3400 cm^{-1} indicates the presence of water molecules. The weak peaks observed at around 3100 cm^{-1} are attributed to the =C-H stretching vibration. Bands at 2900-3000 cm^{-1} are attributed to the vibration of the $–CH_3/–CH_2$. The characteristic bands around 1600 cm^{-1} are assigned to C=N stretching vibration from the bpz*eaT or amino-Schiff-base moiety: 1659 cm^{-1} for **1**, 1657 cm^{-1} for **2** and 1631 cm^{-1} for **3**. The strong bands at 1609, 1457 cm^{-1} for **1**, 1613, 1447 cm^{-1} for **2** and 1627, 1432 cm^{-1} for **3**, respectively, are assigned to asymmetric and symmetric stretching vibrations of the carboxyl group from the tartaric, citric and amino-Schiff ligands. The bands at 991 cm^{-1} for **1**, 997 cm^{-1} for **2** and 953 cm^{-1} for **3** are attributed to the characteristic of V=O stretch, which are similar to those in related complexes.[26] The bands at 945 and 554 cm^{-1} for **1** are assigned to stretching vibration of Op-Op bond and V-Op bonds, respectively. The bands of C-N are observed at 1155, 1060 cm^{-1} for **1**, 1124, 1055 cm^{-1} for **2** and 1148, 1070, 1021 cm^{-1} for **3**. The infrared spectra of the complexes (**1**, **2** and **3**) are consistent with the structural characterization of the complexes **1**, **2** and **3**.

Table 4 IR data (cm^{-1}) for complexes **1-3**.

Complexes	**1**	**2**	**3**
ν(O-H)	3450	3505	3441
ν(=C-H)	3108	3126	3056
ν($-CH_3/-CH_2$)	2979 2930 2881	2980 2940	2919
ν(C=N)	1659	1657	1631
$ν_{as}(COO^-)$	1609	1613	1627
$ν_s(COO^-)$	1490 1457	1486 1447	1432
ν(V=O)	991	997	953
ν(Op-Op)	945	---	---
ν(V-Op)	554	---	---
ν(C-N)	1155 1060	1124 1055	1148 1070 1021

UV-visible spectra

The UV–vis absorption spectra of complexes **1-3** (**Figs. S4-S6**) are recorded in the form of solid samples and their characteristic UV–vis bands are listed in **Table 5**. Bands at 258 nm for **1**, 263 nm for **2** and 265 nm for **3** are attributed to the π-π* transition of the aromatic-like chromophore from the bpz*eaT, 1,10-phen or amino-Schiff-base ligands. Bands at 417 nm for **1** and 388 nm for **2** are assigned to the charge transition from the bpz*eaT ligand to the V(IV) atom, *i.e.* the ligand to metal charge transfer (LMCT) of N→V. Band at 399 nm for **3** is attributed to the charge transition of amino-Schiff-base ligand to the V atom.

Furthermore, the broad peaks at 819 nm for **1**, 584, 764 nm for **2** and 742 nm for **3** are caused by the d-d* transition of the V^{4+} cation.

Table 5 The UV-Vis spectra adscription and comparison for the complexes **1-3**.

Complexes	π→π*/nm	LMCT/nm	d→d /nm
1	258	417	819
2	263	388	584, 764
3	265	399	742

Catalytic activity

Cy oxidation has been reported using homogeneous as well as heterogeneous catalysts.[27-34] Amongst the oxidation products of Cy, CyOH and CyO are important reagents to produce adipic acid and caprolactam that can be used for the manufacture of nylon.[35,36] To explore the new potential catalysts, the catalytic activities of the synthesized complexes (**1-3**) and theirs starting materials ($VO(acac)_2$ and $VOSO_4$) were evaluated in the Cy oxidation with 30% aqueous H_2O_2 as oxidant.

The effect of time was studied when keeping the fixed amount of Cy ($Cy\times10^{-4}$/catalyst molar ratios= 1:1), H_2O_2 ($H_2O_2\times10^{-3}$/catalyst molar ratios= 4.5:1), HNO_3 ($HNO_3\times10^{-3}$/catalyst molar ratios= 1.36:1) and catalyst (0.0004 g) in 3 mL of acetonitrile, at 40 °C. The TONs for CyO/CyOH of complex **1** and its starting material $VO(acac)_2$ were all increased with time on stream as shown in **Fig.4**. It was worth to mention that, the TON values for CyO/CyOH of complex **1** were slightly higher than that of $VO(acac)_2$ before 3h. Beyond that time, complex **1** exhibited much better catalytic activity than $VO(acac)_2$. All the TON values reached the maximum values at 24h, for complex **1**: $TON_{(CyO)}=220$, $TON_{(CyOH)}=346$, $conv_{(Cy)}=97.9\%$ (entry 1, **table 6**) while for $VO(acac)_2$: $TON_{(CyO)}=75$, $TON_{(CyOH)}=186$, $conv_{(Cy)}=93.7\%$ (entry 2, **table 6**). These data clearly show that the catalytic activity of complex **1** is far better than that of its starting material $VO(acac)_2$, which may be primarily due to the peroxo group and more V=O moiety active center in one molecular unit of complex **1** than $VO(acac)_2$.[37]

Similarly, the TONs of complex **3** and its starting material $VOSO_4$ also exhibited increasing trends with time on stream (**Fig. 5**). Unlike the complex **1** and $VO(acac)_2$, the TONs of complex **3** were continuously higher than that of $VOSO_4$ from 1h to 24h (as shown in **table 6**, entry 3-6). This indicates that the oxovanadium Schiff base complex always exhibits high catalytic activity, which is consistent with those reported in the literature.[38]

Comparable were made between complex **1** (entry 1, **table 6**) and **3** (entry 4, **table 6**), which represented that the order of catalytic activity was **1**> **3**, which meant that complex **1** was the best catalyst on Cy oxidation among the **1**, **3**, $VO(acac)_2$ and $VOSO_4$. On the other hand, the structure of complex **2** is similar to complex **1**, which all have V-bpz*eaT moiety. Considered the high activity of complex **1**, complex **2** was applied in the Cy oxidation (entry 7, **table 6**).We were surprised to find that no CyO or CyOH could be detected before 8h, but lots of the target products ($TON_{(CyO)}=88$, $TON_{(CyOH)}=185$, $conv_{(Cy)}=91.1\%$) can be found until the reaction went on to 24h. It may be caused by the peroxo group in complex **1**, which is not existed in complex **2**. A reaction mechanism is also supposed primarily as **Scheme 3**. The complexes converted to [VO(L)(OOH)] (III) by reacting with H_2O_2 to form the transient intermediate [VO(L)(OH)(OOH)] (II) and lost one HO*. It is subsequently transformed to the oxide species (IV) by the loss of one HOO^* radical, which reacts with H_2O_2 to give the species (V). After losing one HO* radical to give the transient intermediate (VI), it immediately converted to the oxide species (VII), which oxidated by H_2O_2 to form the intermediate (VIII). Intermediate species (III) re-back again after species (VIII) losing one molecule of H_2O. In the summary, two HO* and one HOO* radical are generated, together with three H_2O_2 molecules are consumed in this catalytic cycle, which react with Cy to give the corresponding oxidized products. This reaction mechanism is similar to those reported in the literatures which all involved H_2O_2 and generated HO* and HOO* radicals in the catalytic reaction process.[39,40]

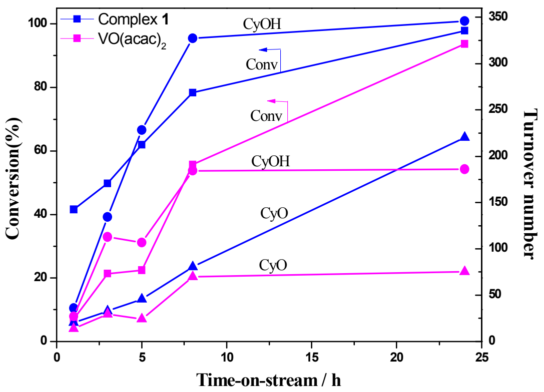

Fig. 4 Effect of the time with complex **1** and $VO(acac)_2$ on the Cy oxidation. Oxidation conditions: n(Cy):n(catalyst) =10000:1, $n(H_2O_2)$:n(catalyst)=4500:1, $n(HNO_3)$: n(catalyst)=1360:1, catalyst (0.0004 g), CH_3CN (3 mL), 40 °C.

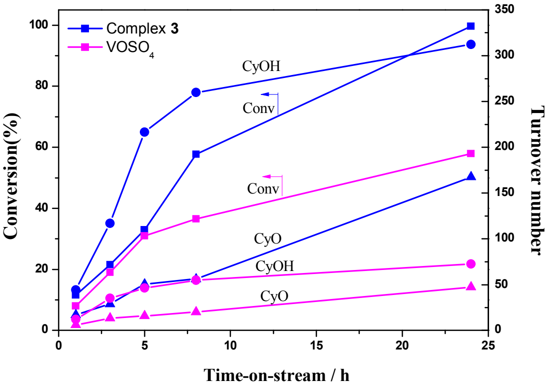

Fig. 5 Effect of the time with complex **3** and $VOSO_4$ on the Cy oxidation. Oxidation conditions: n(Cy):n(catalyst) =10000:1, $n(H_2O_2)$:n(catalyst)=4500:1, $n(HNO_3)$: n(catalyst)= 1360:1, catalyst (0.0004 g), CH_3CN (3 mL), 40 °C.

Table 6 The effect of different catalysts on the Cy oxidation at 24h. Oxidation conditions: n(Cy):n(catalyst) =10000:1, n(H_2O_2):n(catalyst)=4500:1, n(HNO_3): n(catalyst)=1360:1, catalyst (0.0004 g), CH_3CN (3 mL), 40 ^oC.

Entry	complex	t/h	TON (CyO)	TON (CyOH)	Conv. /%
1	**1**	24	220	346	97.9
2	VO(acac)$_2$	24	75	186	93.7
3	**3**	5	50	216	33.0
4	**3**	24	167	312	99.6
5	$VOSO_4$	5	16	46	30.9
6	$VOSO_4$	24	47	72	57.9
7	**2**	24	88	185	91.1

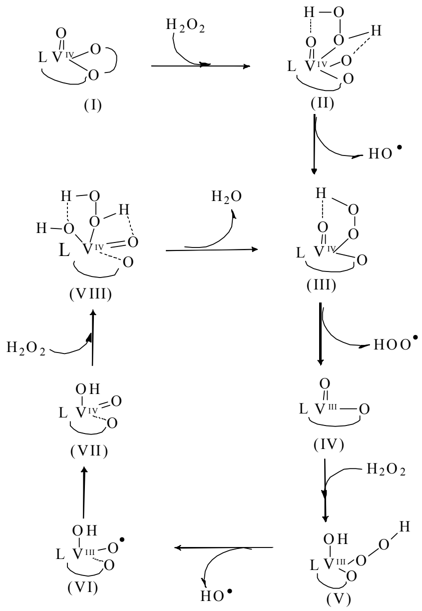

Scheme 3 The key steps of the proposed mechanism of Cy oxidation.

Conclusions

In this work, three new complexes supported by tridentate N-heterocyclic ligands have been successfully synthesized for the first time. The single-crystal X-ray diffraction analyses reveal that the vanadium atoms are six-coordinate in complexes **2** and **3**, while are five- and six-coordinate in complex **1**. 1D chain structures are formed among the molecules in complexes **1** or **3**, while a 2D sheet structure *via* intra- or intermolecular hydrogen bonds are linked in complex **2**. The hydrogen bonds further enhance the structure of the complexes. In the catalytic study, it is found that the three complexes can be considered as potential catalysts, and the order of the catalytic activities are **1**> **3**> VO(acac)$_2$> $VOSO_4$, which means that vanadium complexes with peroxo group, V=O and C=N moiety always exhibit high catalytic activities. Different to the performance that complex **1** is active to the target products all the time, no CyO or CyOH could be detected before 8h catalyzed by complex **2**, which may be caused by the peroxo group. A reaction mechanism of Cy oxidation promoted by vanadium complexes is also supposed primarily.

Supplementary material

The IR spectra and UV–vis spectra are shown in Figs. S1-S6. This material is available free of charge via the Internet at http://pubs.acs.org. Tables of atomic coordinates, isotropic thermal parameters, and complete bond distances and angles have been deposited with the Cambridge Crystallographic Data Center. Copies of this information may be obtained free of charge, by quoting the publication citation and deposition numbers CCDC 1012198 (**1**), 1012730 (**2**) and 1012572 (**3**) from the Director, CCDC, 12 Union Road. Cambridge, CB2 1EZ, UK (fax +44-1223-336033; e-mail deposit@ccdc.cam.ac.uk; http://www.ccdc.cam.ac.uk).

Acknowledgements

We thank the support of this work by the grants of the National Natural Science Foundation of China (No. 21371086 and 21306073), and the science and technology fund for outstanding young talents in Dalian (No.2012J21DW007) for financial assistance.

Notes and references

1 Y. Ishii, S. Sakaguchi and T. Iwahama, *Adv. Synth. Catal.*, 2001, **343**, 393.
2 I. Sökme and F. Sevin, *J. Coll. Interface Sci.*, 2003, **264**, 208.
3 W. Weissermel and H. J. Horpe, *Industrial Organic Chemistry*, 2nd Edn, VCH, Weinheim 1993.
4 A. Ramanathan, M. S. Hamdy, R. Parton, T. Maschmeyer, J. C. Jansen and U. Hanefeld, *Appl. Catal., A: Gen.*, 2009, **355**, 78.
5 D. Alberico, M. E. Scott and M. Lautens, *Chem. Rev.*, 2007, **107**, 174.
6 G. Grivani, V. Tahmasebi, A. D. Khalaji, K. Fejfarová and M. Dušek, *Polyhedron*, 2013, **51**, 54.
7 T. F. S. Silva, T. C. O. M. Leod, L. M. D. R. S. Martins, M. F. C. Guedes da Silva, M. A. Schiavon and A. J. L. Pombeiro, *J. Mol. Catal. A*, 2013, **367**, 52.
8 G. Romanowski, *J. Mol. Catal. A*, 2013, **368**, 137.
9 G. B. Shul'pin, G. S. Mishra, L. S. Shul'pina, T. V. Strelkova and A. J. L. Pombeiro, *Catal. Commun.*, 2007, **8**, 1516.
10 G. B. Shul'pin, Y. N. Kozlov, G. V. Nizova, G. Süss-Fink, S. Stanislas, A. Kitaygorodskiy and V. S. Kulikova, *J. Chem. Soc.*, *Perkin Trans.* 2001, **2**, 1351.
11 Y. N. Kozlov, V. B. Romakh, A. Kitaygorodskiy, P. Buglyó, G. Süss-Fink and G. B. Shul'pin, *J. Phys. Chem. A*, 2007, **111**, 7736.
12 M. Sutradhar, N.V. Shvydkiy, M. F. C. Guedes da Silva, M. V. Kirillova, Y. N. Kozlov, A. J. L. Pombeiro and G. B. Shul'pin, *Dalton Trans.*, 2013, **42**, 11791
13 M. V. Kirillova, M. L. Kuznetsov, P. M. Reis, J. A. L. Silva, J. J. R. F. Silva and A. J. L. Pombeiro, *J. Am. Chem. Soc.*, 2007, **129**, 10531.
14 J.N. Carter-Franklin and A. Butler, *J. Am. Chem. Soc.*, 2004, **126**, 15060.
15 G. Zampella, P. Fantucci, V. L. Pecoraro and L. D. Gioia, *J. Am. Chem. Soc.*, 2005, **127**, 953.
16 J. Elguero, *Comprehensive Heterocyclic Chemistry*, Pergamon: Oxford, 1984.
17 B. Klenke, M. Stewart, M. P. Barrett, R. Brun and I. H. Gilbert, *J. Med. Chem.*, 2001, **44**, 3440.
18 H. S. Patel and V. C. Patel, *Eur. Polym. J.*, 2001, **37**, 2263.
19 X. Wang, Y. H. Xing, F. Y. Bai, X. Y. Wang, Q. L. Guan, Y. N. Hou, R. Zhang and Z. Shi, *RSC Adv.*, 2013, **3**, 16021.

20 C. Chen, Q. Sun, D. X. Ren, R. Zhang, F. Y. Bai, Y. H. Xing and Z. Shi, *CrystEngComm*, 2013, **15**, 5561.

21 A. Guerrero, F. A. Jalon, B. R. Manzano, R. M. Claramunt, P. Cabildo and L. Infantes, *Chem. Heterocycl. Compd.*, 2003, **39**, 1396.

22 D. L. Comins and S. O'Connor, *Adv. Heterocycl. Chem.*, 1988, **44**, 199.

23 H. Y. Zhao, Y. H. Xing, Y. Z. Cao, Z. P. Li, D. M. Wei, X. Q. Zeng and M. F. Ge, *J. Mol. Struct.*, 2009, **938**, 54.

24 G. M. Sheldrick, *SADABS, Program for Empirical Absorption Correction for Area Detector Data*, University of Göttingen, Germany, 1996.

25 G. M. Sheldrick, *SHELXS 97, Program for Crystal Structure Refinement*, University of Göttingen, Göttingen, Germany, 1997.

26 T. A. Alsalim, J. S. Hadi, O. N. Ali, H. S. Abbo and S. J. J. Titinchi, *Chem. Cent. J.*, 2013, **7**, 3.

27 G. Huang, S. Y. Liu, A. P. Wang, Y. A. Guo and H. Zhou, *Catal. Commun.*, 2007, **8**, 1183.

28 H. Einaga and S. Futamura, *Appl. Catal. B*, 2005, **60**, 49.

29 N. Xing, L. T. Xu, F. Y. Bai, H. Shan, Y. H. Xing and Z. Shi, *Inorg. Chim. Acta*, 2014, **409**, 360.

30 L. J. Wan, C. S. Zhang, Z. Li, N. Xing, H. Shan and Y. H. Xing, *Inorg. Chem.*, 2012, **51**, 6517.

31 T. C. O. Mac Leod, M. N. Kopylovich, M. F. C. Guedes da Silva, K. T. Mahmudov and A. J. L. Pombeiro, *Appl. Catal. A*, 2012, **15**, 439.

32 N. Xing, H. Shan, X. Tian, Q. Yao, L. T. Xu, Y. H. Xing and Z. Shi, *Dalton Trans.*, 2013, **42**, 359.

33 D. X. Ren, N. Xing, H. Shan, C. Chen, Y. Z. Cao and Y. H. Xing, *Dalton Trans.*, 2013, **42**, 5379.

34 L. M. D. R. S. Martins, A. Martins, E. C. B. A. Alegria, A. P. Carvalho and A. J. L. Pombeiro, *Appl. Catal. A*, 2013, **464**, 43.

35 A. Pokutsa, O. Fliunt, Y. Kubaj, T. Paczeŝniak, P. Blonarz, R. Prystanskiy, J. Muzart, R. Makitra, A. Zaborovskyi and A. Sobkowiak, *J. Mol. Catal. A*, 2011, **347,** 15.

36 Z. Serinyel, O. Herbinet, O. Frottier, P. Dirrenberger, V. Warth, P. A. Glaude and F. Battin-Leclerc, *Combust. Flame*, 2013, **160**, 2319.

37 H. G. T. Nguyen, M. H. Weston, A. A. Sarjeant, D. M. Gardner, Z. An, R. Carmieli, M. R. Wasielewski, O. K. Farha, J. T. Hupp and S.T. Nguyen, *Cryst. Growth Des.*, 2013, **13**, 3528.

38 G. Grivani, G. Bruno, H. A. Rudbari, A. D. Khalaji, P. Pourteimouri, *Inorg. Chem. Commun.*, 2012, **18**, 15.

39 M. V. Kirillova, M. L. Kuznetsov, V. B. Romakh, L. S. Shul'pina, J. J. R. Fraústo da Silva, A. J. L. Pombeiro and G. B. Shul'pin, *J. Catal.*, 2009, **267**, 140.

40 M. V. Kirillova, M. L. Kuznetsov, Y. N. Kozlov, L. S. Shul'pina, A. Kitaygorodskiy, A. J. L. Pombeiro and G. B. Shul'pin, *ACS Catal.*, 2011, **1**, 1511.